Constraint-based specification of hybrid position-impedance-force tasks

Gianni Borghesan and Joris De Schutter

***Abstract*— This work aims to extend the application field of the constraint-based control framework called iTaSC (*instantaneous task specification using constraints*) toward tasks where physical interaction between the robot and the environment, or a human, is contemplated. iTaSC, in its original formulation, allows for a systematic derivation of control schemes from tasks descriptions; such tasks are defined as constraints enforced on outputs (e.g. distances, angles), and the iTaSC control takes care to fulfil such constraints by computing desired velocities to be commanded to the robot(s) joints. This approach, being based on a velocity resolution scheme, addresses principally tasks where positioning is the main issue. On the contrary, tasks that involve contacts (with the environment or with an user) either desired or accidental, are suited to be carried over taking advantage of impedance control, when position is controlled, or with force control. Here will be described how is possible to realize force tasks, and, by the combination of conflicting force and position tasks, impedance control, within the iTaSC formalism. This result is achieved by taking advantage of an approximate physical modelling of the robotic system and the environment. The proposed control scheme is tested by means of experiments where constraints on forces and/or positions described in cylindrical coordinates are imposed on a Kuka LWR arm.**

I. INTRODUCTION

Focus in robotic research is moving from applications defined in classical industrial settings, where the environment and tasks the robot performs are clearly defined, toward applications where the environment can be partially unknown, and physical interaction with objects, operators, and co-workers, is required, e.g. [1]. These aspects are even more relevant when the robot acts in a household environment: many tasks consist of physical interaction with tools designed for humans [2], or kinematically constrained objects [3].

Tasks with physical interaction are often realized by means of control strategies that involve hybrid force-position control [4], or impedance control, [5]; these two strategies have a 3-decades-long history since the first works date back to the mid ’80s.

On the other hand, iTaSC and other methods derived from the *task function approach* [6] offer several advantages in terms of task description. iTaSC [7] introduced some concepts to ease the description of tasks, namely feature frames and coordinates, and virtual kinematic chains (VKC). These concepts allow to describe the outputs in any (minimal) coordinate system, refereed to any reference systems; iTaSC allows to combine such tasks in order to define more complex tasks; such flexibility has proven to be very useful whenever several tasks are executed concurrently by highly articulated robots [8].

All authors gratefully acknowledge the European FP7 project RoboHow (FP7-ICT-288533).

G. Borghesan, and J. De Schutter are with the Department of Mechanical Engineering, K.U.Leuven, Heverlee, Belgium. name.surname@mech.kuleuven.be

However, iTaSC has been designed for velocity controlled robots, and so most of the applications described in its original formulation focus on positioning tasks. Force control can by achieved with robots equipped with force sensors, as already hinted in [7].

Past works [8]–[10] already made some steps toward extending iTaSC toward physical interaction. In these works had been proposed a way to exploit the back-drivability of robots for defining force tasks in a teleoperation context, without employing force sensing, and force nulling schemes.

In this work, we extend previous results and present them in a harmonized way; the main contributions with respect to the state of art is *to formalize the force and impedance control scheme derivation, so that it is possible to describe hybrid position-impedance-force tasks within the iTaSC framework*.

To reach this objective it is necessary to model the system admittance in the output space, as well as the forces, that are either measured or estimated in Cartesian or joint space.

II. iTASC MODELLING PROCEDURE

An iTaSC application consists of tasks, robots and objects, a scene-graph, and a solver. For every application, the programmer first has to identify the **robots and objects**. In the framework an *object* can be any object in the robot system (for example the robot end-effector, link, or an object attached to it) or in the robot environment. Next, the programmer defines *object frames* $\{o\}$ on the robots and objects (i.e. frames on their kinematic chains) at locations where a task will take effect, for instance the robot end-effector or an object to be tracked.

The actual **tasks** define the space between pairs of object frames ($\{o1\}$ and $\{o2\}$), the *feature space*, as a *virtual kinematic chain (VKC)*. To simplify the task definition, *feature frames* are introduced [7]. The feature frames are linked to an *object*, and indicate a *physical entity* on that object (such as a vertex or surface), or an *abstract geometric property* of a physical entity (such as the symmetry axis of a cylinder). Each task needs at least *two object frames* (called $\{o1\}$ and $\{o2\}$, each attached to one of the objects), and any number of *feature frames* (called $\{f1\}$, $\{f2\}$, $\dots$) For an application in 3D space, there are in general six DOF between $\{o1\}$ and $\{o2\}$. Without loss of generality, we restrict to the case where the six DOF are distributed over six sub-motions, as shown in Fig. 1, i.e. each sub-motion is characterized with a sole degree of freedom.

The general framework allows to account for geometric uncertainties inside kinematic chains of objects or robots, or

$$\begin{tikzcd}
 & \{b^1\} \arrow[r, "\boldsymbol{q}_1"'] & \{o^1\} \arrow[r, "\boldsymbol{\chi}_{fI}"'] & \{f^1\} \arrow[r, "\boldsymbol{\chi}_{fII}"'] & \{f^2\} \arrow[dr, "\boldsymbol{\chi}_{fIII}"] & \\
\{w\} \arrow[ur] & & & & & \{f^3\} \arrow[dl, "\boldsymbol{\chi}_{fIV}"'] \\
 & \{b^2\} \arrow[ul] & \{o^2\} \arrow[l, "\boldsymbol{q}_2"'] & \{f^5\} \arrow[l, "\boldsymbol{\chi}_{fVI}"'] & \{f^4\} \arrow[l, "\boldsymbol{\chi}_{fV}"'] &
\end{tikzcd}$$

Fig. 1: Kinematic task loop with different frames and robot ($\boldsymbol{q}$) and feature ($\boldsymbol{\chi_f}$) coordinates. $\boldsymbol{q}_1$ and $\boldsymbol{q}_2$ are the controllable DOF of the first and second object respectively (typically the robot joints). The feature coordinates $\boldsymbol{\chi_f}$ are the DOF between $\{o1\}$ and $\{o2\}$, which, by introducing the feature frames, are distributed over six submotions: the relative motion of $\{f1\}$ with respect to $\{o1\}$ (submotion I, with feature coordinates $\boldsymbol{\chi_{fI}}$), the relative motion of $\{f2\}$ with respect to $\{f1\}$ (submotion II, with feature coordinates $\boldsymbol{\chi_{fII}}$), *etc.*

virtual kinematic chains. Uncertainties are represented with a minimal set of coordinates in strict analogy with feature coordinates, and are indicated with $\boldsymbol{\chi_{uI}}$, $\boldsymbol{\chi_{uII}}$, *etc.*

The treatment of uncertainties goes beyond the scope of this work and (without loss of generality) will be omitted, considering that all the geometrical properties of objects are known.

At this point, it is necessary to define how the robots and objects are located in the application scene. This is achieved by defining the relations between the reference frames of the robots and objects and a global world reference frame $\{w\}$. By connecting the VKC of the tasks to the object frames on the robots and objects, the programmer defines which robots execute the tasks on which objects. Each task defines a kinematic loop in the scene as shown in Fig. 1.

The kinematic loops introduce constraints between the robot coordinates $\boldsymbol{q}$ and the feature coordinates $\boldsymbol{\chi_f} = \left[\boldsymbol{\chi_{fI}}^T, \boldsymbol{\chi_{fII}}^T, \ldots\right]^T$ expressed by the *loop closure equation*:

$$\boldsymbol{l}\left(\boldsymbol{q}, \boldsymbol{\chi_f}\right) = \boldsymbol{0}, \tag{1}$$

from which is possible to compute the closure loop equation at velocity level:

$$\frac{\partial \boldsymbol{l}\left(\boldsymbol{q}, \boldsymbol{\chi_f}\right)}{\partial \boldsymbol{q}}\dot{\boldsymbol{q}} + \frac{\partial \boldsymbol{l}\left(\boldsymbol{q}, \boldsymbol{\chi_f}\right)}{\partial \boldsymbol{\chi_f}}\dot{\boldsymbol{\chi}}_{\boldsymbol{f}} = \boldsymbol{J_q}\dot{\boldsymbol{q}} + \boldsymbol{J_f}\dot{\boldsymbol{\chi}}_{\boldsymbol{f}} = \boldsymbol{0}, \tag{2}$$

At this point, in order to obtain the desired task behaviour, one has to **impose constraints** on the relative motion between the two objects. To this end, the programmer has to choose the outputs that have to be constrained by defining an *output equation*:

$$\boldsymbol{y} = \boldsymbol{f}\left(\boldsymbol{q}, \boldsymbol{\chi_f}\right) \tag{3}$$

Feature coordinates are usually chosen so that they include the output, and thus $\boldsymbol{f}\left(\cdot\right)$ reduces to selection matrices:

$$\boldsymbol{y} = \boldsymbol{C_q}\boldsymbol{q} + \boldsymbol{C_f}\boldsymbol{\chi_f}, \textit{ and} \tag{4}$$
$$\dot{\boldsymbol{y}} = \boldsymbol{C_q}\dot{\boldsymbol{q}} + \boldsymbol{C_f}\dot{\boldsymbol{\chi}}_{\boldsymbol{f}}. \tag{5}$$

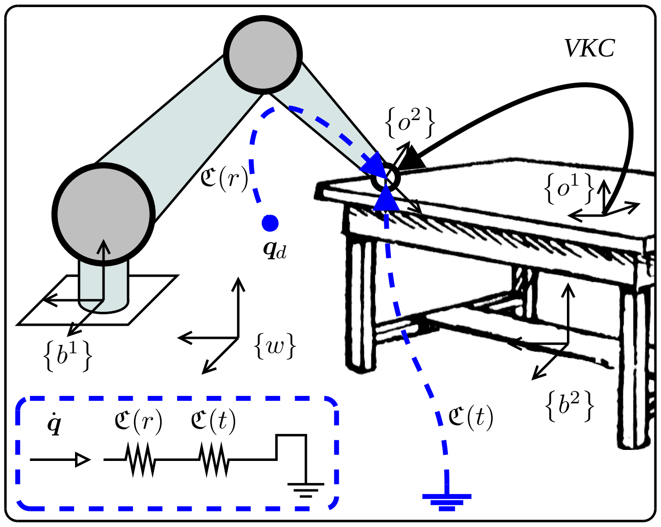

Fig. 2: Compliance of the system: the total compliance of the system is the sum of robot compliance, and the environment compliance. The robot is modelled as spring which stiffness is given by the control gains, and one of the end point is determined by the $\boldsymbol{q}_d$, that in turn is achieved by integration of $\dot{\boldsymbol{q}}$. On the bottom. the equivalent compliance of the system is shown.

The **imposed constraints** used to specify the task are then directly expressed on the outputs as:

$$\boldsymbol{y} = \boldsymbol{y}_d \tag{6}$$

Constraints are enforced by a **controller**, and a **solver**.

The **controller** receives the desired output values ($\boldsymbol{y}_d$) and its derivatives ($\dot{\boldsymbol{y}}_d$) from a *set-point generator*, and computes the desired velocity $\dot{\boldsymbol{y}}_d^\circ$ in the output space:

$$\dot{\boldsymbol{y}}_d^\circ = \boldsymbol{g}\left(\boldsymbol{y}, \boldsymbol{y}_d, \dot{\boldsymbol{y}}_d\right). \tag{7}$$

The **solver** provides a solution for the optimization problem of calculating the desired robot joint values $\dot{\boldsymbol{q}}_d$ from the desired velocities computed by the controller ($\dot{\boldsymbol{y}}_d^\circ$):

$$\dot{\boldsymbol{q}}_d = \boldsymbol{A}_{\boldsymbol{W}}^{\#}\dot{\boldsymbol{y}}_d^\circ, \; \boldsymbol{A} = \boldsymbol{C_q} - \boldsymbol{C_f}\boldsymbol{J_f}^{-1}\boldsymbol{J_q}. \tag{8}$$

This allows us to weight differently conflicting constraints (over-constrained case), and to weight the effort actuation cost at joint velocity level (under-constrained case).

III. From Force Constraints Specification to Force Control

The typical implementation of (7) is

$$\dot{\boldsymbol{y}}_d^\circ = \boldsymbol{K}_p(\boldsymbol{y}_d - \boldsymbol{y}) + \dot{\boldsymbol{y}}_d \tag{9}$$

This control, in the hypothesis that (*i*) the system composed by the robot and its low level control is able to follow the desired joint velocities, and (*ii*) there are no conflicting tasks, achieves perfect tracking, after a transition time which duration is ruled by the gain matrix $\boldsymbol{K}_p$.

As already shown in [7] and other works, in a velocity resolved scheme, reference forces cannot be imposed directly, but must be translated into displacement.

Let the generalized forces exerted by the robot be defined as $\boldsymbol{\tau_y}$; in order to compute the desired velocity to be actuated from desired force, the admittance of the system must be considered:

$$\delta \boldsymbol{y} = \boldsymbol{a}\left(\boldsymbol{\tau_y}\right) \tag{10}$$

A very good trade-off for (10) is to consider compliance, i.e. a linear, quasi-static approximation of $\boldsymbol{a}\left(\cdot\right)$:

$$\delta \boldsymbol{y} = \mathfrak{C}_{\boldsymbol{y}} \boldsymbol{\tau_y} \tag{11}$$

Where $\mathfrak{C}_{\boldsymbol{y}}$ is the total compliance of the system, and the subscript y indicates that it is expressed in the output space; how to compute such compliance is the focus of next paragraph.

A. Compliance of the kinematic loop

The system represented in Fig. 2 shows a typical example of tasks that includes physical interaction. The robot and the table are characterized by a compliance matrix, that is coordinate-dependent. For the sake of simplicity, we will make the assumption that the compliance depends only on the robot joints: this hypothesis implies that (*a*) the low level controller of the robot is a proportional joint position controller, and (*b*) the environment is characterized by linear compliance, that does not depend on the objects configuration (e.g. fixed, not articulated objects).

In the condition shown in Fig. 2 we have two compliances. Let the robot be driven with the following law:

$$\boldsymbol{\tau_q} = \boldsymbol{K}_q(\boldsymbol{q}_d - \boldsymbol{q}) + \boldsymbol{B}(\dot{\boldsymbol{q}}) + \boldsymbol{G}(\boldsymbol{q}) \tag{12}$$

where $\boldsymbol{\tau_q}$ is the torque commanded at joint level, and $\boldsymbol{q}_d$ is obtained by integration of $\dot{\boldsymbol{q}}_d$, computed by (9).

Then, assuming that the robot joints and links mechanical compliance is negligible w.r.t. the control compliance, the compliance of the robot object in joint space can be approximated as:

$$\mathfrak{C}_{\boldsymbol{q}}(r) \approx \boldsymbol{K}_q{}^{-1} \tag{13}$$

In other words, *the robot behaves as a spring in which one side is determined by* $\boldsymbol{q}_d$.

On the other side, the compliance of the object is expressed in some reference frame, (*e.g.* $\{o^1\}$) w.r.t. some application point. With simple operations, it can be expressed in any frame and any application points. For sake of simplicity, let us consider the compliance of the object (table in Fig. 2) $\mathfrak{C}^{o1,o1}(t)$ be expressed in Cartesian coordinates $\{o1\}$ and applied in $\{o1\}$.

When the robot is pushing on the object, in absence of slipping or tilting, we can consider that they are fixed together i.e. the object frame $\{o1\}$ attached to one object $o1$ (the table), and the frame $\{o2\}$ attached to $o2$ (the robot) cannot experience relative movements.

In this situation, the compliances sums together (as shown at the bottom of Fig. 2), but in order to numerically compute it, all compliances must be represented in the same space and expressed in the same coordinate system, for example we can decide to represents all compliances in $\{o2\}$ and applied in $\{o2\}$. Then, the robot compliance is:

$$\mathfrak{C}^{o2,o2}(r) = \boldsymbol{J}_{\boldsymbol{r}o2,o2}\, \mathfrak{C}_{\boldsymbol{q}}(r)\, \boldsymbol{J}_{\boldsymbol{r}o2,o2}^T \tag{14}$$

where $\boldsymbol{J}_{\boldsymbol{r}o2,o2}$ is the Jacobian that maps joint velocities in the twist expressed and applied in $\{o2\}$. The compliance for the object table, supposing that the object original compliance is given in $\{o1\}$, can be computed as:

$$\mathfrak{C}^{o2,o2}(t) = \mathbf{Ad}(\boldsymbol{T}_{o2}^{o1})\mathfrak{C}^{o1,o1}(t)\mathbf{Ad}(\boldsymbol{T}_{o2}^{o1})^T \tag{15}$$

where $\mathbf{Ad}(\boldsymbol{T}_{o2}^{o1})$ is the Adjoint matrix (see among others [11]) that maps twists expressed/applied in $\{o1\}$ to twists expressed/applied in $\{o2\}$.

Following this guideline, it is possible to express all compliances in a common frame and combine them in $\mathfrak{C}^{o2,o2}$,

$$\mathfrak{C}^{o2,o2} = \mathfrak{C}^{o2,o2}(r) + \mathfrak{C}^{o2,o2}(t). \tag{16}$$

However, the final goal is to control the system in the output space, therefore the whole system compliance must be represented in such space.

B. Representing the system compliance in the feature and output space

Equations (2) and (5) contain the relations that are necessary for computing compliance in the output space: from $\boldsymbol{J_f}$, the Jacobian of the virtual kinematic chain, it is possible to compute $\boldsymbol{J_f}_{o2,o2}$,the Jacobian expressed/applied in $\{o2\}$, and consequently:

$$\mathfrak{C}_{\boldsymbol{f}} = \boldsymbol{J}_{\boldsymbol{f}o2,o2}^{-1}\mathfrak{C}^{o2,o2}\boldsymbol{J}_{\boldsymbol{f}o2,o2}^{-T} \tag{17}$$

where $\mathfrak{C}_{\boldsymbol{f}}$ is the compliance expressed in the feature space and coordinates, and so relates the generalised positions and the generalised forces $\boldsymbol{\tau_f}$.

Finally, it is possible to compute the compliance in the output space, for the given example:

$$\mathfrak{C}_{\boldsymbol{y}} = \boldsymbol{C_f}\mathfrak{C}_{\boldsymbol{f}}\boldsymbol{C_f}^T + \boldsymbol{C_q}\mathfrak{C}_{\boldsymbol{q}}\boldsymbol{C_q}^T. \tag{18}$$

Thanks to (18), it is possible to relate forces and position/velocities in the output space, and also which is the desired displacement in order to achieve a desired force.

The last factor that is needed for implement a force feedback law are the force measurements, *i.e.* the force that are applied by the robot, either measured or estimated. How to express such forces in the output space is the topic of the next paragraph.

C. Force sensing

In order to close the loop over a desired force, the iTaSC controller must be able to measure the force in the output space. Force measurements can be achieved directly, by means of force sensors mounted on the robot, or in case the robot is back-drivable, the force applied by the robot on the environment can be approximated by a function of the force exerted by the motors. Independent of the space (joint or Cartesian) where the force is sensed or estimated, it must be represented/applied in a way that is uniform with the compliance representation: the output space.

Following the same rationale used for compliance computation, measured forces are represented as wrenches $\boldsymbol{w}_{o2,o2}$ expressed/applied in $\{o2\}$, that could be measured directly (by equipping the robot with a force sensor in such point) or computed indirectly from measured torques:

$$\boldsymbol{w}_{o2,o2} = \boldsymbol{J}_{\boldsymbol{r}o2,o2}^{-T} \boldsymbol{\tau_q} \tag{19}$$

Lastly, for each task, the measured wrench is expressed in feature and then output space:

$$\boldsymbol{\tau_f} = \boldsymbol{J}_{\boldsymbol{f}o2,o2}^{T} \boldsymbol{w}_{o2,o2}, \tag{20}$$

$$\boldsymbol{\tau_y} = \boldsymbol{C_q}^{-T} \boldsymbol{\tau_q} + \boldsymbol{C_f}^{-T} \boldsymbol{\tau_f}. \tag{21}$$

At this point all the necessary elements to describe the extended iTaSC controller are present.

IV. The force-position-impedance controller

Section IV shows how to: *a*) formalize a control equation that regulates forces, *b*) how to combine such equation with position constraints in order to realize an impedance behaviour, and *c*) how to cope with partial modelling of the physical properties of the scene, and which is the expected behaviour in contact and free space.

A. Constraint-based force control

We would like to extend the control equation (7) in such a way it includes generalized forces. The typical implementation of the controller shown in (9) has the nice property that the matrix $\boldsymbol{K}_p$ has as unit $[1/\mathrm{s}]$ independently of which is the unit of the output (e.g. $[\mathrm{m}]$ or $[\mathrm{Rad}]$). Since $\boldsymbol{K}_p$ is normally chosen as a diagonal matrix, the total system behaves as a set of first order systems whose settling time is ruled by $\boldsymbol{K}_p$ (under the assumptions that the robot executes the commanded velocity, and there are no conflicting constraints).

This property can be maintained by relating force errors to position errors:

$$\dot{\boldsymbol{y}}_d^{\circ} = \boldsymbol{K}_p \mathfrak{C}_{\boldsymbol{y}} (\boldsymbol{\tau_{y}}_d - \boldsymbol{\tau_y}) + \mathfrak{C}_{\boldsymbol{y}} \dot{\boldsymbol{\tau}}_{\boldsymbol{yd}} \tag{22}$$

where $\boldsymbol{\tau_{y}}_d$ and $\dot{\boldsymbol{\tau}}_{\boldsymbol{yd}}$ are the desired forces and their first derivative.

Supposing that the modelled compliance is a good approximation of the real system, the position error is related to the force error by the compliance matrix;

$$\mathfrak{C}_{\boldsymbol{y}} (\boldsymbol{\tau_{y}}_d - \boldsymbol{\tau_y}) = (\boldsymbol{y}_d - \boldsymbol{y}), \tag{23}$$

and hence (22) and (23) will have the same time evolution.

B. Constraint-based impedance control

Combining position and force constraints enables the imposition of compliance behaviour. Let $\boldsymbol{W}$ be a diagonal matrix containing normalised weights:

$$\boldsymbol{W} = \mathrm{diag}(w_1, \dots),\ w_i \in [0, 1]. \tag{24}$$

Let us consider as outputs generalised positions and forces that are expressed in the same space, *i.e.* derived from the same virtual kinematic chain and selected by the same selection matrices $\boldsymbol{C_f}$ and $\boldsymbol{C_q}$; then, the composition of the two in the same equation results in:

$$\begin{aligned} \dot{\boldsymbol{y}}_d^{\circ} =& (\boldsymbol{1} - \boldsymbol{W}) \left(\boldsymbol{K}_p (\boldsymbol{y}_d - \boldsymbol{y}) + \dot{\boldsymbol{y}}_d \right) \\ &+ \boldsymbol{W} \left(\boldsymbol{K}_p \mathfrak{C}_{\boldsymbol{y}} (\boldsymbol{\tau_{y}}_d - \boldsymbol{\tau_y}) + \mathfrak{C}_{\boldsymbol{y}} \dot{\boldsymbol{\tau}}_{\boldsymbol{yd}} \right) \end{aligned} \tag{25}$$

Where the gain matrices $\boldsymbol{K}_p$ have been chosen purposefully the same (in order to achieve the desired time evolution of the error), and $\boldsymbol{\tau_{y}}_d$, $\dot{\boldsymbol{\tau}}_{\boldsymbol{yd}}$ are the desired force and its first derivative.

The static behaviour of (25) is:

$$(\boldsymbol{1} - \boldsymbol{W})(\boldsymbol{y}_d - \boldsymbol{y}) = -\boldsymbol{W} \mathfrak{C}_{\boldsymbol{y}} (\boldsymbol{\tau_{y}}_d - \boldsymbol{\tau_y}), \tag{26}$$

from which the stiffness that is achieved by the controller can be computed:

$$\boldsymbol{K} = (\boldsymbol{1} - \boldsymbol{W})\, \boldsymbol{W}^{-1} \mathfrak{C}_{\boldsymbol{y}}^{-1}. \tag{27}$$

Each output stiffness can vary from infinite (pure position control) to null (pure force control), depending by the value of w_i, effectively allowing to choose the behaviour of the system, in each of the output directions, independently.

Note that the stiffness $\boldsymbol{K}$ can be shaped either by choosing the $\boldsymbol{W}$ matrix, or $\mathfrak{C}_{\boldsymbol{y}}$, which in turn is related to the gain stiffness of the low level controller, (12). We preferred to choose the matrix $\boldsymbol{K}_q$ as a diagonal matrix, instead of decoupling the compliance matrix in the outputs space, because: *a*) the robot could execute multiple tasks at once, each one with different coordinates, and so it would be unclear which task to use for computing $\boldsymbol{K}_q$, and *b*) even if one task in feature space is used, if the robot is redundant (like the robot used in the experiments), and in general when the number of controlled directions in the output space is smaller than the number of actuated joints, the matrix $\boldsymbol{K}_q$ will have a null space, resulting in the impossibility to actuate a given velocity is some direction of the joint space, thus preventing tasks described in joint space to be executed correctly.

V. Effects of inexact modelling and free-space behaviour of force control

As highlighted in the introductory section, iTaSC is often used in applications where the environment is partially unknown. Normally, the compliance of the robot in contact situation is dominated by (12), and can be considered known with good approximation. If the object which the robot interacts with is flexible, it will have a non-null compliance, and so the total compliance will increase, along with the feed-back gain $\boldsymbol{K}_p \mathfrak{C}_{\boldsymbol{y}}$ and feed-forward constant $\mathfrak{C}_{\boldsymbol{y}}$ of (22). This can be interpreted in the following way: in order to achieve the same force, the more the object is compliant, the bigger will be the needed compression.

In case the compliance is overestimated, the feed-forward will overcompensate, and the time constant will be reduced. On the contrary, an underestimation will increase the settling time, allowing for safer interaction, at a cost of performance: in most of the cases, the objects are rigid and their compliance can be neglected.

If the robot is not in contact, from a modelling point of view, the compliance of the kinematic loop degenerates

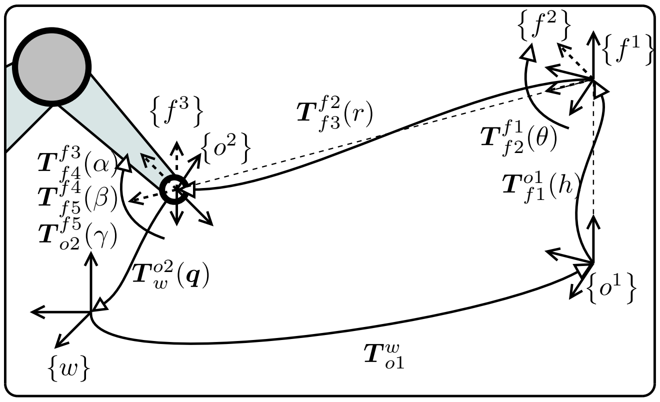

$\{f^2\}$
$\{f^1\}$
$\{f^3\}$
$\boldsymbol{T}_{f3}^{f2}(r)$
$\{o^2\}$
$\boldsymbol{T}_{f2}^{f1}(\theta)$
$\boldsymbol{T}_{f4}^{f3}(\alpha)$
$\boldsymbol{T}_{f5}^{f4}(\beta)$
$\boldsymbol{T}_{f1}^{o1}(h)$
$\boldsymbol{T}_{o2}^{f5}(\gamma)$
$\boldsymbol{T}_{w}^{o2}(\boldsymbol{q})$
$\{o^1\}$
$\{w\}$
$\boldsymbol{T}_{o1}^{w}$

Fig. 3: Representation of the virtual kinematic chain employed in the experiments. It consists in a cylindrical coordinates system, with $\boldsymbol{\chi}_f = (h, \theta, r, \alpha, \beta, \gamma)$. In figure are reported the object frames $\{o^1\}$ and $\{o^2\}$ and the first 3 feature frames, $\{f^1\}$, $\{f^2\}$, $\{f^3\}$. The other 2 feature frames, $\{f^4\}$, $\{f^5\}$, omitted for the sake of clarity, have the origin in common with $\{o^2\}$. Arrows with empty head represent transformations $\boldsymbol{T}(\cdot)$, that can be constant, ($\boldsymbol{T}_{o1}^{w}$), dependent of joint coordinates ($\boldsymbol{T}_{w}^{o2}(\boldsymbol{q})$), or by the feature coordinates ($\boldsymbol{T}_{o2}^{o1}(\boldsymbol{\chi}_f)$).

Exp	pos.	imp.	for.	HRI/Free/Contact	Figure
1	h, θ, r			HRI	Fig. 4
2	r	h, θ		HRI	Fig. 5
3	r		h, θ	HRI	Fig. 6
4	h, θ, r			Free Space	Fig. 7a
5	r	h, θ		Free Space	Fig. 7b
6	θ, r		h	Contact	Fig. 8

TABLE I: List of presented experiments: In the first 3 experiments, the robot is pushed by a person, with fixed desired position and desired forces. In the exp. 4 and 5, the robot follows a *position trajectory* without contacts, and in the last one a *force trajectory* while in contact with a rigid object.

toward infinity, since no force can be achieved with any displacement: clearly this condition cannot be accounted for, and the compliance is modelled as if the robot is always in contact.

This choice, as can be inferred by (22), causes the systems to behave as a pure damper with damping constant:

$$\boldsymbol{B} = (\boldsymbol{K}_p \mathfrak{C}_{\boldsymbol{y}})^{-1}. \tag{28}$$

VI. Experimental evaluation

In order to illustrate the behaviour of the proposed approach, a number of experiments have been carried over. All experiments employ the same virtual kinematic chain, that is anchored in a fixed position above a table from one side, and at the robot end-effector on the other side; the transformation between the base frame of the robot $\{b^2\}$ and the object one $\{o^1\}$ is fixed:

$$\boldsymbol{T}_{o1}^{w} = \left[\begin{array}{c|c} & -1 \\ \boldsymbol{1}_{3\times3} & 0 \\ & 0.5 \\ \hline \boldsymbol{0}_{3\times1} & 1 \end{array}\right] \tag{29}$$

The robot used in the experiment is the KUKA LWR arm, a seven dof arm equipped with torque sensors mounted at each joint, while the VKC is designed to resemble cylindrical-like coordinate, and so is build using the following transformations: *i*) TransZ, *ii*) RotZ, *iii*) TransY, *iv*) RotX, *v*) RotY, and *vi*) RotZ. Each transformation is done w.r.t. its local frame, as shown in Fig. 3, and each one is parametrized by one of the feature coordinates:

$$\boldsymbol{\chi_f} = (h, \theta, r, \alpha, \beta, \gamma)$$

The first 3 coordinates are the cylindrical coordinates, while the last 3 angles represent the 3 DoF rotation that brings $\{f^3\}$ to $\{o^2\}$.

As output is chosen the whole feature space, $\boldsymbol{C_f} = \boldsymbol{1}$, and no joint variables, $\boldsymbol{C_f} = \emptyset$. For all experiments, we control the last four variables (radius and relative pose) in position, with a fixed value: so $\{o^2\}$ (the robot end-effector) is commanded to maintain a constant distance w.r.t. the z-axis of $\{o^1\}$ and the end-effector is always facing the above mentioned axis. The other two degrees of freedom are set both in position ($w_i = 0$), impedance ($w_i = 0.8$), or force ($w_i = 1$), and the system is either pushed and released by a user, left in free space, or in contact with a rigid object, while the desired output values are commanded with a trajectory (free-space and hard-contact case) or kept constant (human interaction case). As a general rule, when impedance control is used, the force reference in that output direction is kept null. The experiments that have been carried over are resumed in Table I.

A. Physical interaction with user: exp. 1,2, and 3

The first set of experiment that is proposed shows the behaviour of the robot when an user exerts force on it. Three possibilities are tested: All output controlled in position (Fig. 4), the outputs h and θ controlled with the impedance strategy (Fig. 5), or controlled in force (Fig. 6), where the force reference in the last two cases is null. The expected behaviour is that:

- in the first case the iTaSC controller brings to zero the error, trying to compensate for all disturbances,
- in the second, the user experiences a spring like behaviour, but is constrained to a cylindrical surface, while
- in the latter case, the robot behaves as a damped system, that, again is constrained to move on the cylinder surface.

From Fig. 4 it possible to appreciate the position accuracy, that is around $1\,\mathrm{cm}$, and the dynamics that the robot shows while recovering the reference position. Note that in static condition the position controller has infinite stiffness, since the iTaSC controller behaves as integral controller, on top of the low level proportional controller. In case a deviation

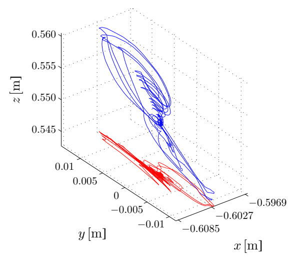

(a) Trajectory of $o2$ expressed in the robot base; in red, projection of trajectory in the $x-y$ plane.

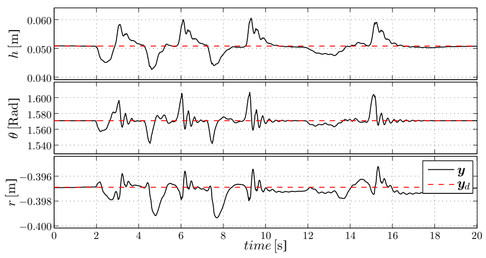

(b) Output (gen. position)

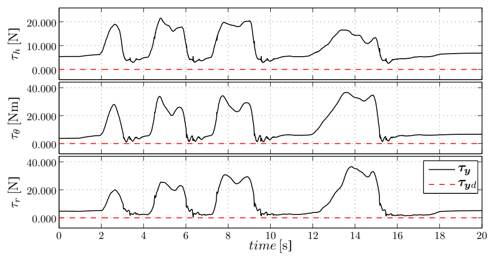

(c) Output (generalised forces)

Fig. 4: Experiment N.1: all degrees of freedom are controlled in position.

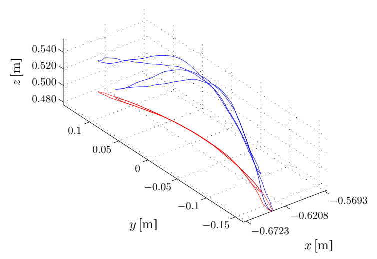

(a) Trajectory of $o2$ expressed in the robot base; in red, projection of trajectory in the $x-y$ plane.

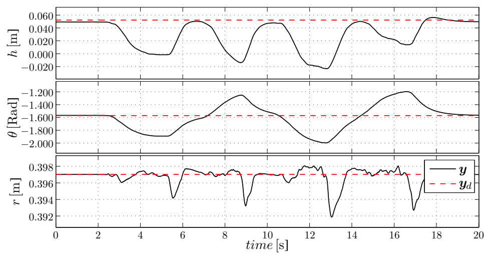

(b) Output (gen. position)

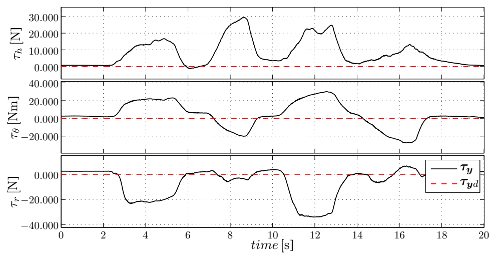

(c) Output (generalised forces)

Fig. 5: Experiment N.2: Output h and θ are controlled with impedance.

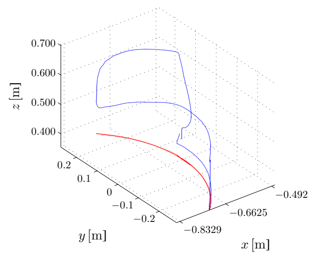

(a) Trajectory of $o2$ expressed in the robot base; in red, projection of trajectory in the $x-y$ plane.

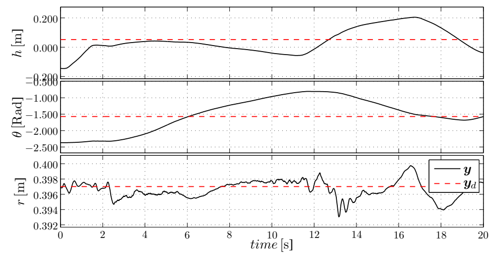

(b) Output (gen. position)

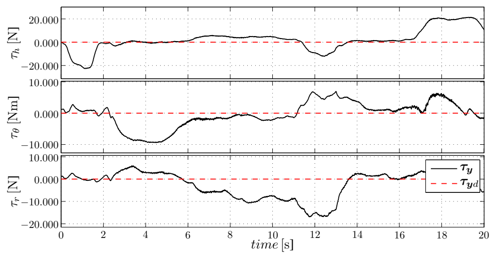

(c) Output (generalised forces)

Fig. 6: Experiment N.3: Output h and θ are controlled in force, (with a null reference force).

from original position is maintained for a long period, the controller will continue increasing the torque. For this reason, this kind of control is not safe and predictable when unforeseen collisions could happen.

In the second experiment, the impedance control is tested. The weights for the first two output is set to 0.8. This translate to the physical stiffness described by (27). The user pushes the robot (that is constrained on the cylinder surface, whose axis is along the z-axis, and its origin is in $(-1, 0, 0.5)[\mathrm{m}]$). When the robot is released (i.e. when estimated torques diminishes in Fig. 5c), it goes back to the rest position, roughly following a first order dynamics in each of the output space, as shown by Fig. 5b.

The third experiment shows instead the force controller behaviour. Now the user is free to steer the robot end-effector on the cylinder surface, experiencing a force that is proportional to the velocity that he imposes to the robot, as ruled by (28). In Fig. 6a. it is possible to appreciate the cylinder surface.

It is worth noticing that due to the kinematics of the virtual kinematic chain, for the same positions two solution exists, one with positive r (e.g.Figs 5 and 6), or negative r (Fig. 4), that is mainly determined by the initialization of the inverse kinematic algorithm that solve the loop closure, (1).

B. *Position control in free space: exp. 4,5*

Another set of two experiments shows how the system behaves in free space. In this case, the robot is commanded to move along an arc of circle. The same movement is performed with all outputs controlled in position, and with

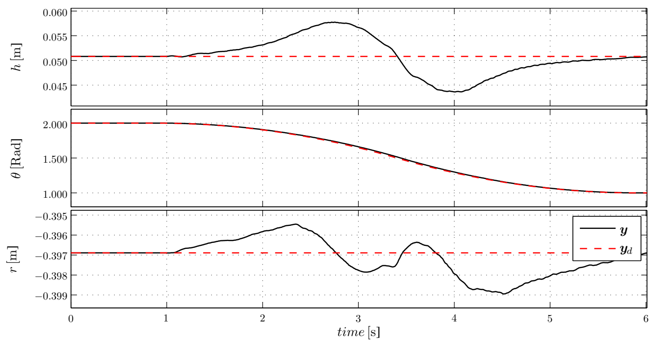

(a) Experiment 3, all outputs in position control.

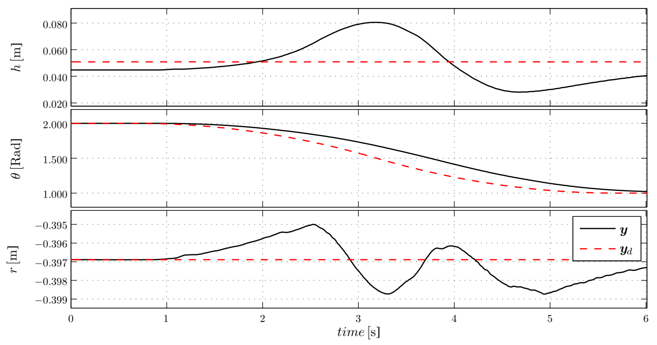

(b) Experiment 4, outputs θ and h in impedance control (with null desired output torques).

Fig. 7: Experiment N. 3 and 4: The output θ is commanded to follow a trapezoidal velocity profile of time length $t = 5\,\mathrm{s}$, from $\theta_1 = 2\,\mathrm{Rad}$ from $\theta_2 = 1\,\mathrm{Rad}$.

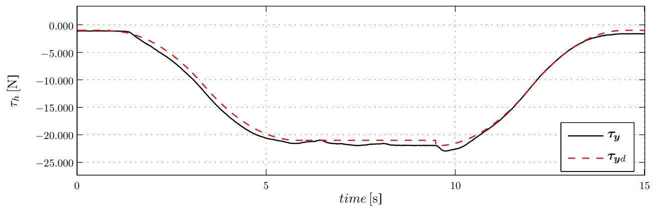

Fig. 8: Experiment N. 6: The output τ_h is commanded to follow two trapezoidal velocity profiles of time length $t = 5\,\mathrm{s}$ each: from $-1\,\mathrm{N}$ from $-21\,\mathrm{N}$, and *vice-versa*.

h and θ in impedance mode. Fig. 7 allows to compare the two experiments; as expected, the position control (Fig. 7a) behaves better, during the movement (negligible tracking error), and in steady state (steady state error tends to zero). The impedance controller, instead shows a phase lag: since the force measured by the robot joint sensor is influenced by links inertia, sudden movements conflicts with the zero force constraint. However, the degradation of performance can be acceptable when unexpected contacts are possible. Note that, in case forces would have been measured by a force sensor on the end-effector (or any other means to discern which are the forces due to inertia from forces due to contact is used), the system would behave as in the first case.

C. Force control in contact situation, exp. 6

Lastly, a contact situation is presented. In this case the robot is commanded to exert a force on a table, starting from a contact situation. The desired force profile is composed by two trapezoidal profiles, from $-1\,\mathrm{N}$ to $-21\,\mathrm{N}$, and *vice-versa*. These profiles are characterized by the reference force and its derivative, as requested by the control equation (22).

The other degrees of freedom are commanded in position (i.e. the robot can move only along h), and since the h direction is physically constrained by the table that is very stiff, the robot does not move significantly.

Being the table compliance negligible, assuming as total compliance the compliance of the robot control is an accurate hypothesis, and reflects on the good force tracking shown in Fig. 8. In this case it can be observed that the feed-forward term is dominant w.r.t. the feedback, as the error in the second part of the trajectory is very reduced, while in the first five seconds the robot is actually anticipating a little the desired value.

VII. Final remarks

In this work, a systematic way to formalize hybrid position-impedance-force control has been presented, along with some experiments to show the behaviour. In the authors opinion, the method allows to cope with a number of tasks where contact situation are sought, expected, or possible. This method has been designed specifically to be used with iTaSC, but can be easily extended to any method where the control is solved at velocity level, so long a Jacobian that maps output velocity to the control variable is computed, either by means of geometrical relations, analytically, or numerically.

On the other side, we did not make any assumption on which is the method for measuring the force, so long is it possible to compute the force applied on the origin of the object frame attached to the robot.

We did not mention, for the sake of brevity, other characteristics of the iTaSC framework, for example the treatment of geometric uncertainties, and the possibility to execute tasks where both objects are robots (e.g. bi-manual manipulation). This contribution has been thought taking in mind these aspects as well, and so it can be integrated with minimal effort in a complete iTaSC controller.

References

[1] S. Haddadin, M. Suppa, S. Fuchs, T. Bodenmller, A. Albu-Schffer, and G. Hirzinger, "Towards the robotic co-worker," in *Robotics Research*, ser. Springer Tracts in Advanced Robotics, C. Pradalier, R. Siegwart, and G. Hirzinger, Eds. Springer Berlin Heidelberg, 2011, vol. 70, pp. 261–282.

[2] C. C. Kemp, A. Edsinger, and E. Torres-Jara, "Challenges for Robot Manipulation in Human Environments," *IEEE Robotics & Automation Magazine*, vol. 14, no. March, pp. 20–29, 2007.

[3] C. Ott, B. Bauml, C. Borst, and G. Hirzinger, "Employing cartesian impedance control for the opening of a door: A case study in mobile manipulation," in *IFAC Symposium on Intelligent Autonomous Vehicles*, 2007.

[4] O. Khatib, "A unified approach for motion and force control of robot manipulators: The operational space formulation," *IEEE Journal on Robotics and Automation*, vol. 3, no. 1, pp. 43–53, Feb. 1987.

[5] N. Hogan, “Impedance control: An approach to manipulation, parts i-iii,” *Transactions of the ASME, Journal of Dynamic Systems, Measurement, and Control*, vol. 107, pp. 1–24, 1985.

[6] C. Samson, M. Le Borgne, and B. Espiau, *Robot Control, the Task Function Approach*. Oxford, England: Clarendon Press, 1991.

[7] J. De Schutter, T. De Laet, J. Rutgeerts, W. Decre, R. Smits, E. Aertbelin, K. Claes, and H. Bruyninckx, “Constraint-based task specification and estimation for sensor-based robot systems in the presence of geometric uncertainty,” *International Journal of Robotic Research*, vol. 26, no. 5, pp. 433–455, 2007.

[8] D. Vanthienen, T. De Laet, W. Decré, H. Bruyninckx, and J. De Schutter, “Force-Sensorless and Bimanual Human-Robot Comanipulation Implementation using iTaSC,” in *Proc. of 10th IFAC Symposium on Robot Control*, 2012, pp. 832–839.

[9] G. Borghesan, B. Willaert, T. De Laet, and J. De Schutter, “Teleoperation in Presence of Uncertainties : a Constraint-Based Approach,” in *Proc. of 10th IFAC Symposium on Robot Control*, 2012, pp. 385–392.

[10] G. Borghesan, B. Willaert, and J. De Schutter, “A constraint-based programming approach to physical human-robot interaction,” in *IEEE Proc. of the Int. Conf. on Robotics and Automation*, 2012.

[11] R. M. Murray, Z. Li, and S. S. Sastry, *A Mathematical Introduction to Robotic Manipulation*, C. Press, Ed., 1994.